Physics Faculty Research & Creative Works   Physics

01 Jan 1990

Binary Nucleation Of Ethanol And Water

John L. Schmitt
Missouri University of Science and Technology, jschmitt@mst.edu

J. Whitten

G. W. Adams

R. A. Zalabsky

Binary nucleation of ethanol and water ⊘

J. L. Schmitt; J. Whitten; G. W. Adams; R. A. Zalabsky

Check for updates

View Online   Export Citation   CrossMark

Binary nucleation of ethanol and water

J. L. Schmitt, J. Whitten,[a] G. W. Adams,[b] and R. A. Zalabsky[c]

Physics Department and Graduate Center for Cloud Physics Research, University of Missouri-Rolla, Rolla, Missouri 65401

The authors have used a fast expansion cloud chamber to measure binary homogeneous nucleation rates in several ethanol–water mixtures as a function of temperature, ethanol and water activities and nucleation rate. Data (ethanol and water activities) are presented for a range in nucleation rate from 10^3 to 10^5 drops/cm^3 s from 263 to 293 K for mixtures having mole ratios (ethanol/water) of 10, 4, 0.1, 0.01, and 0.001. A comparison of the extensive data set to other data in the literature shows good agreement. We find current theory, as expected, is unable to accurately predict the data at low ethanol concentrations.

INTRODUCTION

In this work we have measured the activities, as a function of temperature, composition and nucleation rate, required for the binary homogeneous nucleation of mixtures of ethanol and water (E–W) in argon in a fast-expansion Wilson cloud chamber. We did this work in order to produce an extensive set of experimental data to test current and future theoretical descriptions of binary homogeneous nucleation. Ethanol and water were selected as materials for this investigation for several reasons: they are both very common materials and therefore there is general interest in them and the literature contains information, e.g., thermodynamics constants, on them; they form a strongly interacting mixture and thus interpretation of the measurements presents a significant test of theory and, finally, the E–W system already has had some nucleation experiments performed on it and has been investigated theoretically.

Since there are recent reviews of binary homogeneous nucleation theory, Mirabel and Jaecker-Voirol[1] and Wilemski,[2] with references to the E–W system, we only will briefly review the subject here. Reiss[3] in 1950 published the first complete treatment of binary nucleation based on previous homogeneous nucleation theory. Doyle[4] applied that theory to sulfuric acid in 1961. Experimentally, Flood[5] obtained nucleation data in an expansion chamber on E–W in 1934. Although E–W mixtures were extensively used in the Wilson cloud chamber for the detection of nuclear particle tracks (Das Gupta and Gnosh[6]) the first quality binary nucleation data was obtained by Mirabel and Katz[7] in 1977 with a diffusion chamber. The Mirabel and Katz data clearly demonstrated that the then existing classical theory was inadequate to describe E–W, particularly at low ethanol concentrations (high water activity).

The crucial parameter in binary nucleation is the free energy of formation. A correct calculation of the free energy requires knowledge of the composition of the critical cluster and in the case of E–W appears to require knowledge of the

critical cluster surface. It is widely believed that the surface of an E–W cluster can have a considerably different composition than the bulk. At low ethanol concentrations there is a very significant surface enrichment of ethanol. Wilemski[2,8] has briefly reviewed the theories that currently attempt to describe binary homogeneous nucleation: Reiss[3]; Doyle[4]; Flageollet-Daniel, Garnier, and Mirabel[9]; Rasmussen[10]; Spiegel, Zahoransky, and Wittig[11]; and Wilemski.[12]

Below we present our extensive measurements of binary homogeneous nucleation in several mixtures of E–W over a wide range of temperature, ethanol and water activity and nucleation rate.

EXPERIMENTAL PROCEDURE

Our measurements on E–W were made with a precision Wilson expansion cloud chamber. This chamber is continually being improved, particularly in its electronic control apparatus, but its basic construction and operational details are as previously discussed in Refs. 13 and 14. The chamber previously was used to measure the homogeneous nucleation of ethanol, toluene, nonane, and styrene (Refs. 15–18). These references also contain further details about our chamber and, in particular, contain the methods and rationale for calculating the supersaturation and nucleation temperature from the initial temperature, initial pressure and peak (actually a minimum) expansion pressure. This work has used a similar technique to calculate the ethanol activity, water activity and nucleation temperature by the straightforward addition of a second condensable vapor in the calculations.

REDUCTION OF THE DATA

Approximately 1200 data expansions were made with the expansion chamber for this work. Our first step in calculating the nucleation rate from the raw chamber data was to examine each separate data set by plotting a graph of ethanol or water activity vs drop count. Separate data sets are usually one day's experiments with the chamber. Data sets for the same temperature and mole ratio were then compared; incorrect points were discarded and the sets combined. Figure 1 is the composite plot for one of these combined sets and contains all points for ethanol activity vs drop count for an

[a] Presently at U.S. Army, TRADOC Analysis Command, Ft. Leavenworth, Kansas 66027.

[b] Presently at Center for Naval Analyses, 4401 Ford Avenue, P.O. Box 16268, Alexandria, Virginia 22302-0268.

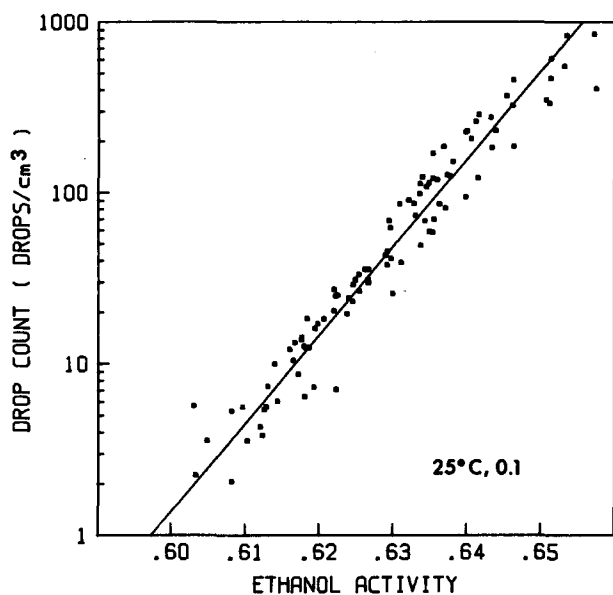[c] Presently at P.O. Box 81, Pittsville, Wisconsin 54466.

FIG. 1. The drop count in the expansion chamber as a function of ethanol activity for an initial temperature of 25 °C and a (E/W) mole ratio of 0.1.

FIG. 2. The experimental drop count and nucleation rate as a function of ethanol and water activity. The E/W liquid mixture mole ratio is 0.001. See the text for further details.

initial chamber temperature of 25 °C and a liquid pool mixture mole ratio of 0.1.

Separate plots were made for both ethanol activity vs drop count and water activity vs drop count at each temperature and composition. At first, one may think that ethanol activity and water activity are independent variables and that one would analyze the data on a three-dimensional surface. In general for theory this is correct, but in practice, in an adiabatic expansion the variables ethanol activity, water activity and drop count create a curved line in three dimensions rather than a surface and ethanol activity and water activity are functions of each other (for an expansion). The function joining them is a complex one, but nonetheless it is single valued for an expansion. We have therefore simplified the analysis by treating ethanol activity vs drop count and water activity vs drop count separately.

Each of the ethanol or water vs drop count data sets was fitted with a least squares fit. Each data set with its fitted curve was individually plotted and examined to assure that the curve indeed did fit well, represent physical reality and, if necessary, extrapolate properly. The curve in Fig. 1 shows such a fit to that data set. One should note that in Fig. 1 the curve has been extrapolated to the full range of 1–1000 drops/cm³. For each data set the fit was used to calculate the E–W activities required to produce 1–1000 drops/cm³.

The results from the least squares fits to the data are plotted in Figs. 2–6. Each graph represents the data for one mixture mole ratio (the ratio of the number of moles of ethanol to the number of moles of water in the liquid pool in the chamber). The solid curves in these graphs show the E–W activities required to produce from 1–1000 drops/cm³ for an expansion from the given initial temperature. Near each curve is the initial chamber temperature, in degrees Centigrade, followed by a rough average of the peak temperature, the temperature at which nucleation took place, in degrees Kelvin. The nucleation temperature varies somewhat along
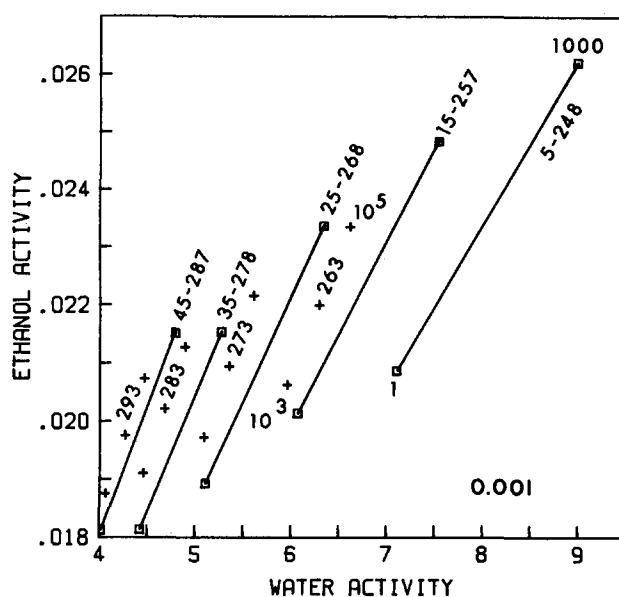
these curves due to the varying depth of expansion, from the fixed initial temperature, required to produce varying nucleation counts (drops/cm³). Figures 2–6 exhibit the range of initial temperature, nucleation temperature for the mixtures, and nucleation rate covered by the data.

One must analyze the drop count (drops/cm³) as function of time to determine the nucleation rate (drops/cm³ s). If our expansion chamber were able to expand infinitely fast, one could experimentally produce a pressure (nucleation) pulse that descended to the nucleation pressure in an infinitely short time, stayed only at that pressure and ascended
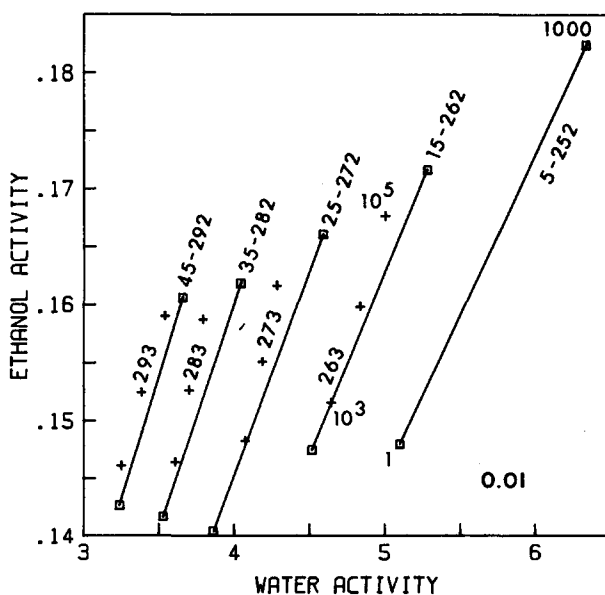

FIG. 3. The experimental drop count and nucleation rate as a function of ethanol and water activity. The E/W liquid mixture mole ratio is 0.01. See the text for further details.

FIG. 4. The experimental drop count and nucleation rate as a function of ethanol and water activity. The E/W liquid mixture mole ratio is 0.1. See the text for further details.

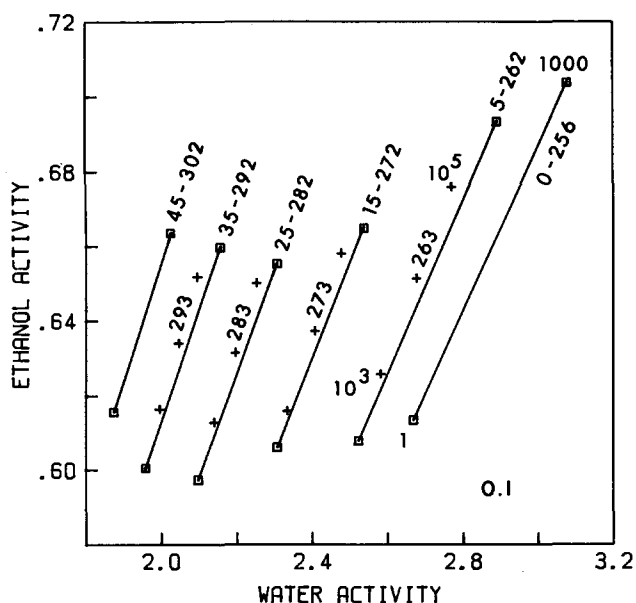

FIG. 6. The experimental drop count and nucleation rate as a function of ethanol and water activity. The E/W liquid mixture mole ratio is 10. See the text for further details.

again infinitely fast. In this imaginary rectangular pulse case, all the nucleation would take place at the same pressure (equivalently: supersaturation or activity) for a known length of time and the nucleation rate ideally would be the drop count divided by the time. For example, for an interval of 0.01 s and a drop count of 134 drops/cm^3 the nucleation rate would be 13 400 drops/cm^3 s. Obviously our chamber is a real mechanical system and does not operate this way. Therefore we have proceeded, as in the past, Ref. 17, by measuring the actual pressure pulse (pressure as a function of time, see below) in the chamber and integrating over it.
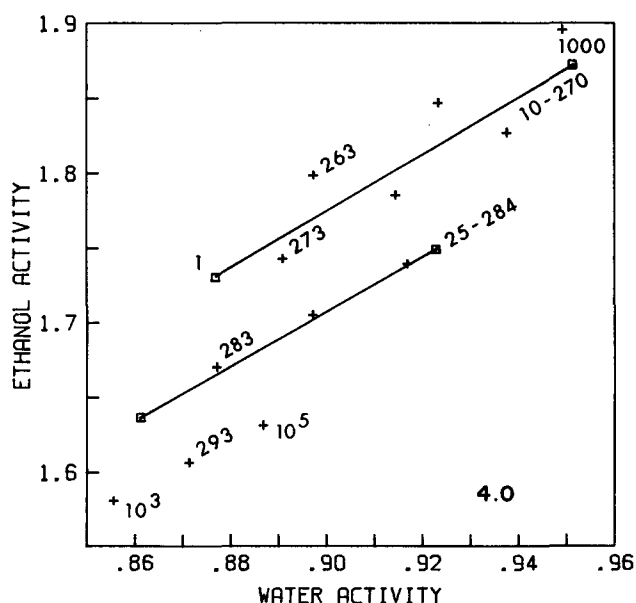
The pressure pulse shape for the chamber has been very consistent from expansion to expansion over the years the chamber has been in operation. It is given, as in previous work, by

$$P(t) = P_{\min} + 1.143t + (3.3945 \times 10^5)t^2, \qquad (1)$$

where $0.01 \geqslant t \geqslant -0.01$ s (t is measured from the peak of the pulse, t is in s and P is in mmHg).

We proceed as follows: The pressure as a function of time is used to calculate the activities as a function of time near and at the peak. The least squares fit to each data set provides us with an empirical nucleation count equation (activity vs drop count). We then integrate over the pulse using our empirical count equation and normalize to the experimental drop count. The nucleation rate is then found by dividing by the integration time interval.

We have found from a series of these calculations that

$$J = KC, \qquad (2)$$

where J is the nucleation rate, K is a (average) constant for each temperature and mole fraction and C is the drop count from the data. We have examined the nucleation rate predicted by this simple relationship and find that it is within $\pm 5\%$ of the value determined by an integration over the nucleation pulse for representative data points (over the initial temperature range from $+45$ to 0 °C) at a given mole ratio. The variation of K as a function of mole ratio is about $\pm 15\%$ over the range of mole ratio in this work. We therefore have calculated and used separate constants for each mole ratio. Hung *et al.*[19] independently found a similar relationship when analyzing nonane data from our chamber.

Theoretical calculations for binary nucleation have as their goal the prediction of the nucleation rate as a function of activities and temperature. To facilitate a comparison with theory we have used our average experimental data to find nucleation rates at several temperatures. The average

FIG. 5. The experimental drop count and nucleation rate as a function of ethanol and water activity. The E/W liquid mixture mole ratio is 4. See the text for further details.
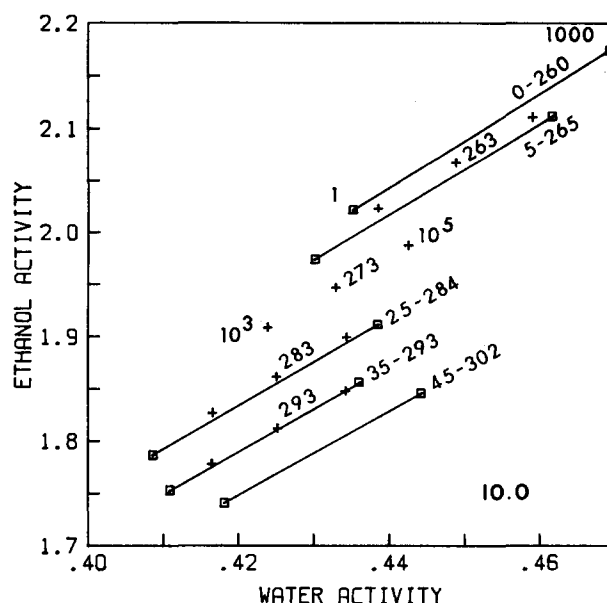
experimental activities (along the curves) exhibited in Figs. 2–6 are all at different temperatures, and thus we treated this data with a multidimensional least squares fit which allows us to calculate the activities required to nucleate 10^3, 10^4, and 10^5 drops/cm^3 s [nucleation rate as found from Eq. (2)] at 263.15, 273.15, 283.15, and 293.15 K. In most cases this is an interpolation but, some extrapolation has been made. These calculated values are plotted as crosses in Figs. 2–6. The crosses are in groups of three, each group corresponding to the indicated temperature in degrees Kelvin; in each group the crosses correspond to 10^3, 10^4, and 10^5 drops/cm^3 s nucleation rate. The numerical values (E–W activities) used to plot these crosses are listed in Table I to facilitate use of our results by other investigators.

Figures 7–10 exhibit the ethanol activity and water activity at constant nucleation rates of 10^3, 10^4, and 10^5 drops/ cm^3 s for all experimental mixture mole ratios at 263.15, 273.15, 283.15, and 293.15 K. The points plotted (labeled SWAZ) are those from Table I and previously exhibited in Figs. 2–6 in graphs of much higher resolution. Also in Figs. 7–10, plotted as points, are homogeneous nucleation data on pure ethanol (water activity = 0) and pure water (ethanol activity = 0). The pure ethanol data are from Ref. 15, with the exception that the pure ethanol point (at 10^3 drops/cm^3 s) in Fig. 10 is extrapolated from data in Kacker and Heist.[20] The pure water data are from Miller.[21,22]

Schmitt *et al.*[15] and Strey, Schmeling and Wagner[23] found anomalous behavior for the homogeneous nucleation of pure ethanol. Specifically, contrary to expectation, a higher supersaturation was required to nucleate at 45 °C (initial temperature) than at 25 °C. Strey *et al.*[23] have proposed that this is an effect of association during the expansion of the expansion chamber and that during the expansion there is a release of latent heat due to the association. We have not performed experiments that are specifically designed to test the practical effects of this process, but we have noticed the following effects in our data which may apply to this question.

Anomalous nucleation does not seem to be present in the data for a mole ratio of 10 (10 moles of ethanol to 1 mole
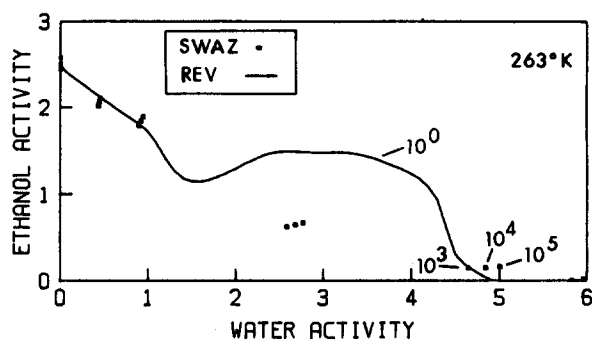

FIG. 7. The ethanol and water activities measured at 263 K that yield nucleation rates of 10^3, 10^4, and 10^5 drops/cm^3 s (our work, SWAZ). The solid curve is calculated from the revised nucleation theory for 1 drop/cm^3 s nucleation rate.

of water) exhibited in Figs. 6 and 10. In Fig. 6 the 45 °C data does not follow the other data well, but it also does not exhibit the drastic anomaly (reversal) observed in pure ethanol. Even more important, in Fig. 10 one notes that the data points (for a mole ratio of 10) agree well with the diffusion chamber data for which there should be no effect. The effect should manifest itself as an increase in the activities (as presented) as opposed to the "real" activities with the association effect included. This is not seen as a noticeable effect in Fig. 10. For these reasons and the lack of information on the energies for the process in E–W, we have not attempted to include association effects in the reduction of our data.

It is readily apparent when one reduces raw data that the computations critically depend on the thermodynamic parameters used in the calculations. We therefore list the parameters we used in Table II.

The activity coefficients for the temperature and mole fraction range of the experimental data were obtained by interpolation and extrapolation of coefficients found in the literature. The principal source of information is the work of d'Avila and Silva.[24] However that work covers only from 30 to 10 °C and 0.1 to 0.9 mole fraction of ethanol. Additional data was taken from sources in Ref. 25 for an extension to

TABLE I. Experimental ethanol and water activities as a function of temperature and nucleation rate for several mixture mole ratios.

| Mole ratio (E/W) Temp.	Rate	Pure Eth.	10 Eth.	Water	4 Eth.	Water	0.1 Eth.	Water	0.01 Eth.	Water	0.001 Eth.	Water	Pure Water
263 K	10^3	2.454	2.023	0.439	1.799	0.897	0.626	2.581	0.152	4.650	0.0206	5.957	5.824
	10^4	2.515	2.067	0.449	1.847	0.923	0.651	2.677	0.160	4.843	0.0220	6.298	6.115
	10^5	2.582	2.111	0.459	1.895	0.949	0.676	2.770	0.167	5.005	0.0233	6.618	6.445
273 K	10^3	2.429	1.909	0.424	1.743	0.890	0.616	2.334	0.148	4.074	0.0197	5.087	5.048
	10^4	2.500	1.947	0.433	1.785	0.914	0.637	2.407	0.155	4.191	0.0210	5.356	5.291
	10^5	2.582	1.988	0.443	1.827	0.938	0.658	2.477	0.161	4.286	0.0222	5.609	5.568
283 K	10^3		1.827	0.417	1.670	0.877	0.613	2.139	0.146	3.608	0.0191	4.456	4.456
	10^4		1.862	0.425	1.705	0.897	0.631	2.196	0.153	3.706	0.0202	4.680	4.677
	10^5		1.899	0.434	1.739	0.917	0.650	2.253	0.159	3.799	0.0213	4.894	4.932
293 K	10^3	2.26	1.778	0.416	1.581	0.856	0.616	1.995	0.146	3.251	0.0183	4.064	3.991
	10^4		1.812	0.425	1.606	0.871	0.634	2.045	0.152	3.386	0.0198	4.269	4.215
	10^5		1.848	0.434	1.631	0.887	0.651	2.096	0.159	3.543	0.0207	4.472	4.481
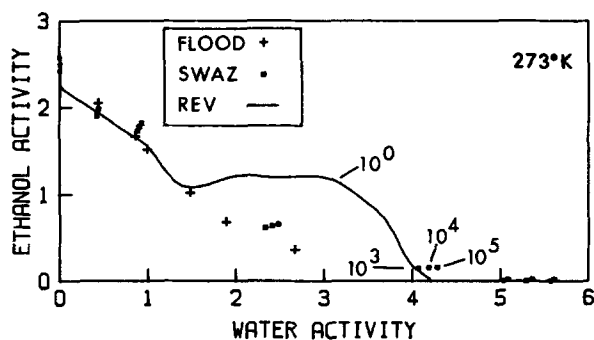
FIG. 8. The ethanol and water activities measured at 273 K that yield nucleation rates of 10^3, 10^4, and 10^5 drops/cm^3 s (our work, SWAZ). The crosses exhibit Flood's data at 2 drops/cm^3 s (Ref. 5). The solid curve is calculated from the revised nucleation theory for 1 drop/cm^3 s nucleation rate.
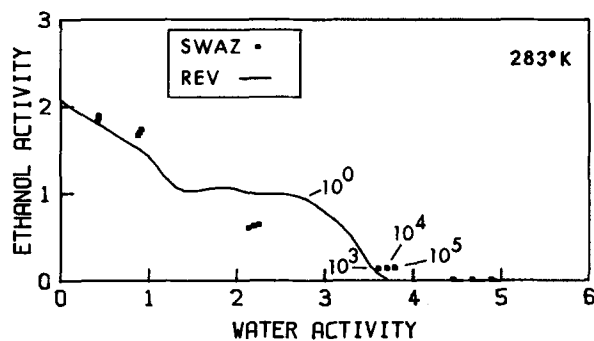

FIG. 9. The ethanol and water activities measured at 283 K that yield nucleation rates of 10^3, 10^4, and 10^5 drops/cm^3 s (our work, SWAZ). The solid curve is calculated from the revised nucleation theory.
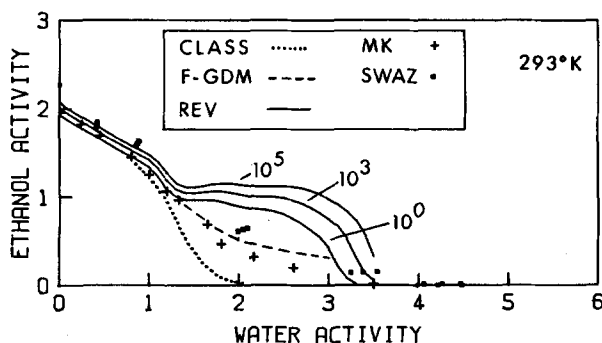

FIG. 10. The ethanol and water activities measured at 293 K that yield nucleation rates of 10^3, 10^4, and 10^5 drops/cm^3 s (our work, SWAZ) The Mirabel and Katz work (MK, Ref. 7) is at 1 drop/cm^3 s. The curves show various theoretical predictions, see the text.

TABLE II. Thermodynamic parameters.

Ideal gas heat capacities (ergs/mol K)[a]

$$C_{p1} = 1.928 \times 10^9 (0.131\,22 + 9.185\,66 \times 10^{-4}T$$

$$- 2.359\,57 \times 10^{-7}T^2 - 7.191\,65 \times 10^{-11}T^3)^b$$

$$C_{p2} = 2.0776 \times 10^8 \ ^b$$

$$C_{p3} = 7.541\,08 \times 10^8 (0.452\,219 - 1.292\,24 \times 10^{-4}T$$

$$+ 4.170\,08 \times 10^{-7}T^2 - 2.004\,01 \times 10^{-10}T^3)^b$$

Saturation vapor pressure (dyn/cm^2)

$$\ln(P_{e1}/P_c) = 1/T_r [- 8.456\,573\,9(1 - T_r)$$

$$+ 0.090\,430\,576(1 - T_r)^{1.5}$$

$$- 4.834\,83(1 - T_r)^3 + 3.761\,077\,9(1 - T_r)^6]$$

where $T_r = T/513.92$ and $P_c = 6137$ KPA^c

$$P_{e3} = 6.107\,799\,961 + 0.443\,651\,852T + 1.428\,9458\,05 \times 10^{-2}T^2$$

$$+ 2.650\,648\,471 \times 10^{-4}T^3 + 3.031\,240\,396 \times 10^{-6}T^4$$

$$+ 2.034\,080\,948 \times 10^{-8}T^5 + 6.136\,820\,929 \times 10^{-11}T^{6\ d}$$

where T is in °C

Second virial coefficients (cm^3/mol)

$$B_1(T) = 672.4761(0.155\,595\,9 - 0.26008/T_r - 0.2145/T_r^2$$

$$- 0.026\,843\,98/T_r^3 - 0.110\,959\,9 \times 10^{-2}/T_r^8),$$

where $T_r = T/516.3^e$

$$B_2(T) = - 1150.935 + 20.7692T - 0.167\,822\,3T^2$$

$$+ 0.712\,531\,2 \times 10^{-3}T^3$$

$$- 0.154\,184\,1 \times 10^{-5}T^4 + 0.134\,154\,2 \times 10^{-8}T^{5\ f}$$

$$B_3(T) = 243.3141(0.145\,229\,9 - 0.325\,399/T_r$$

$$- 0.1435/T_r^2 - 0.013\,07/T_r^3 - 0.729\,999\,4 \times 10^{-4}/T_r^8)$$

where $T_r = T/647.3^e$

Liquid density (gm/cm^3)

$$d_1 = 1.034\,061 - 0.836\,809 \times 10^{-3}T^g$$

$$d_3 = - 2.101\,73 + 25.4641\,9T_r - 82.809\,28T_r^2$$

$$+ 134.8906T_r^3 - 111.1521T_r^4 + 36.654\,53T_r^{5\ h}$$

where $T_r = T/647.3$

Activity coefficients, partial molar volumes, and surface tensions, see the text.

[a] Subscript 1 refers to ethanol, 2 to argon, and 3 to water.

[b] Y. S. Touloukian and T. Makita, *Thermophysical Properties of Matter: Vol. 6, Specific Heat* (IFI/Plenum, New York, 1970).

[c] B. D. Smith and R. Scrivastava, *Thermodynamic Data for Pure Compounds, Part A: Hydrocarbons and Ketones* (Elsevier, New York, 1986).

[d] P. R. Lowe and J. M. Ficke, ENVPREDRSCHFAC Technical Paper No. 4-74 (Naval Postgraduate School, Monterey, 1974). A polynomical fit to values from J. A. Goff and S. Gratch, Trans. Amer. Soc. Heat. Vent. Eng. 52, 95 (1946).

[e] Dr. Buford Smith, Department of Chemical Engineering, Washington University, St. Louis, MO (private communication, 1978).

[f] From fit of points in *The Thermodynamic Properties of Argon from The Triple Point to 300 K at Pressures to 1000 Atmospheres* (National Bureau of Standards, Washington, 1969).

[g] Thermodynamics Research Center, *Selected Values of Properties of Hydrocarbons and Related Compounds* (Texas A&M University, College Station, Texas, 1965).

[h] From fit of points in *Smithsonian Meteorological Tables, 6th ed.*, prepared by R. J. List (Smithsonian Inst., Washington, D.C., 1968).

higher temperatures and values were taken for ethanol activity coefficients at infinite dilution from Refs. 26 and 27. We found no data in the literature at temperatures lower than 10 °C and thus we extrapolated the existing data using the functional form:

$$\ln \gamma = C + D/T, \tag{3}$$

where γ is the activity coefficient and C and D are constants, as suggested on page 263 of Ref. 28 (for constant mole fraction). In practice the activities were calculated by first fitting selected data to Eq. (3), a functional dependence on only temperature, at several mole fractions. At the desired temperature we calculated the ethanol activity coefficient for several mole fractions. We then fit a fifth order polynomical to those activity coefficients to allow us to calculate the ethanol and water activity coefficients directly from the Hansen–Miller equations (Ref. 29, see also Ref. 26). Partial molar volumes were computed by standard physical chemistry textbook techniques from the E–W densities as a function of percent weight found in Refs. 30 and 31. Surface tensions were taken from the work of Teitlebaum *et al.*[32] as cited in Ref. 31.

COMPARISON WITH OTHER MEASUREMENTS AND THEORY

Previous experimental work on E–W nucleation has been performed by Flood[5] at approximately 270–280 K in an expansion chamber, Mirabel and Katz[7] at 293 K with a diffusion chamber and Spiegel, Zahoransky, and Wittig[11] at 270–290 K with a shock tube. Flood's data for a nucleation rate of about 2 drops/cm^3 s (taken from Ref. 7) are plotted in Fig. 8. With the exception of the point at high ethanol activity, the data agrees well with our data at much higher nucleation rates. The Mirabel and Katz data (MK) for 1 drop/cm^3 s are shown as crosses in Fig. 10. The agreement between the data sets is quite good, both show the same general shape of the curve and the progression from 1 (their data) to 10^3, 10^4, 10^5 drops/cm^3 s (our data), on the scale of this graph, appears correct. Figure 11 further exhibits our data at 10^5 drops/cm^3 s over the temperature range 273–293 K and the data of Zahoransky and Wittig[33] at 10^{10}
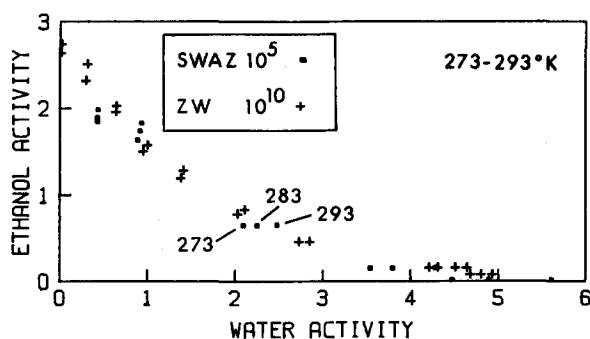
drops/cm^3 s from 270–290 K (taken from the plot in Ref. 12). The Zahoransky and Wittig data are above our data at high ethanol activities and are within the range of our data at lower ethanol activities; because of the wide range in nucleation temperature it is difficult to make a more detailed comparison. Measurements by Zahoransky and Peters[34] are at temperatures lower than 263.15 K and therefore have not been included in our comparison.

We examined current theory in the literature and concluded that the revised standard theory as detailed in Ref. 12 offered the advantages of computational simplicity and a published fit to existing E–W data. The solid curves in Figs. 7–9 (labeled REV) show the result of our computations for 1 drop/cm^3 s using the revised theory. Similar computations yielded the additional curves shown in Fig. 10 for 10^3 and 10^5 drops/cm^3 s. In addition the classical theory prediction, taken from Ref. 12, and the F-DGM[9] results are shown in Fig. 10 (labeled CLASS and F-GDM, respectively). The F-DGM prediction from the literature is obviously the best fit to the data even though it too deviates at low ethanol concentrations. Since the F-DGM theory pays particular attention to the properties of the cluster surface, it would appear that further work should carefully incorporate the nature of this surface. One also may have to take into account the changing nature of the E–W liquid structure as a function of mole fraction, Onori.[35]

Finally, with the addition of our data to that already in the literature, we now have experimental measurements of the binary nucleation of E–W over a wide range of temperature, ethanol and water activities and nucleation rate. However, it is obvious if one considers the large change in nucleation rate that occurs with a small change in activity (see the high resolution graphs: Figs. 2–6), that low resolution graphs such as Fig. 10 do not constitute a stringent test of theory.

CONCLUSIONS

We have measured an extensive body of data on the binary nucleation of ethanol and water mixtures. The data cover the temperature range 263 to 293 K for nucleation rates from 10^3 to 10^5 drops/cm^3 s. Data were obtained at liquid mixture mole ratios (ethanol/water) of 10, 4, 0.1, 0.01, and 0.001. If we compare our data, primarily at 293 K, with existing data from the literature at 1 drop/cm^3 s nucleation rate, we find good agreement. The simple comparison of our data set with theoretical predictions shows most discrepancy at low ethanol concentrations.

FIG. 11. The ethanol and water activities measured by us (SWAZ), 10^5 drops/cm^3 s, and Zahoransky and Wittig (ZW, Ref. 33), 10^{10} drops/cm^3 s, in the temperature range 270–293 K.

[1]P. Mirabel, and A. Jaecker-Voirol, in *Lecture Notes in Physics, Vol. 309: Atmospheric Aerosols and Nucleation*, edited by P. Wagner and G. Vali (Springer, Berlin, 1988), p. 3.

[2]G. Wilemski, in *Lecture Notes in Physics, Vol. 309: Atmospheric Aerosols and Nucleation*, edited by P. Wagner and G. Vali (Springer, Berlin, 1988), p. 367.

[3]H. Reiss, J. Chem. Phys. **18**, 840 (1950).

[4]G. J. Doyle, J. Chem. Phys. **35**, 795 (1961).

[5]H. Flood, Z. Phys. Chem. A **170**, 286 (1934).

[6]N. N. Das Gupta and S. K. Gnosh, Rev. Mod. Phys. **18**, 225 (1946).

[7]P. Mirabel and J. Katz, J. Chem. **67**, 1697 (1977).

[8]G. Wilemski, J. Chem. Phys. **88**, 5134 (1988).

[9]C. Flageollet-Daniel, J. P. Garnier, and D. Mirabel, J. Chem. Phys. **78**, 2600 (1983).

[10]D. W. Rasmussen, J. Chem. Phys. **85**, 2272 (1986).

[11]G. H. Spiegel, R. A. Zahoransky, and S. Wittig, in *Shock Waves and Shock Tubes*, edited by D. Bershaden and R. Hanson (Stanford University, Stanford, 1986), p. 775.

[12]G. Wilemski, J. Phys. Chem. **91**, 2492 (1987).

[13]J. L. Schmitt, Rev. Sci. Instrum. **52**, 1749 (1981).

[14]J. L. Schmitt, J. L. Kassner, Jr., and J. Podzimek, J. Aerosol Sci. **13**, 373 (1982).

[15]J. L. Schmitt, G. W. Adams, and R. A. Zalabsky, J. Chem. Phys. **77**, 2089 (1982).

[16]J. L. Schmitt, R. A. Zalabsky, and G. W. Adams, J. Chem. Phys. **79**, 4496 (1983).

[17]G. W. Adams, J. L. Schmitt, and R. A. Zalabsky, J. Chem. Phys. **81**, 5074 (1984).

[18]J. L. Schmitt, J. Chem. Phys. **89**, 5307 (1988).

[19]C. Hung, M. Krasnopoler, and J. Katz, J. Chem. Phys. **90**, 1856 (1989).

[20]A. Kacker and R. Heist, J. Chem. Phys. **82**, 2734 (1985).

[21]R. Miller, Ph.D. dissertation, University of Missouri-Rolla, Rolla, Missouri, 1976.

[22]R. Miller, R. Anderson, J. L. Kassner, Jr., and D. Hagen, J. Chem. Phys. **78**, 3204 (1983).

[23]R. Strey, T. Schmeling, and P. Wagner, J. Chem. Phys. **85**, 6192 (1986).

[24]S. G. d'Avila and R. S. F. Silva, J. Chem. Eng. Data, **15**, 421 (1970).

[25]J. Gmehling and A. Onken, *Vapor–Liquid Equilibrium Data Collection*, Vol. 1, pt. 1 DECHEMA, Frankfurt, 1977).

[26]L. Nord, E. E. Tucker, and S. D. Christian, J. Soln. Chem. **13**, 849 (1984).

[27]R. C. Pemberton and C. J. Mash, J. Chem. Therm. **10**, 867 (1978).

[28]R. C. Reid, J. M. Prausnitz, and B. E. Poling, *Properties of Gases and Liquids*, 4th ed. (McGraw–Hill, New York, 1987).

[29]R. S. Hansen and F. A. Miller, J. Phys. Chem. **58**, 193 (1954).

[30]C. J. West and C. Hull, *International Critical Tables*, Vol. III (McGraw–Hill, New York, 1933), p. 116.

[31]J. Timmermans, *Physico-Chemical Constants of Binary Systems*, Vol. 4 (Interscience, New York, 1960), p. 197.

[32]B. Y. Teitelbaum, T. A. Gortalowa, and E. Siderova, Zh. Fiz. Khim. **25**, 911 (1951).

[33]R. A. Zahoransky, and S. Wittig, in *Proceedings of the 13th International Symposium on Shock Tubes and Waves: Niagara Falls,* 1981, edited by C. E. Treanor and J. G. Hall (SUNY Press, Albany, 1982), p. 682.

[34]R. A. Zahoransky and F. Peters, J. Chem. Phys. **83**, 6425 (1985).

[35]G. Onori, J. Chem. Phys. **89**, 4325 (1988).